

Structural and optical characterization of PVP-capped lead oxide nanocrystalline thin films

S. C. EZUGWU^{a*}, P. U. ASOGWA^a, F. I. EZEMA^a, P. M. EJIKEME^b

^a*Department of Physics and Astronomy, Faculty of Physical Sciences, University of Nigeria, Nsukka*

^b*Department of Chemistry, Faculty of Physical Sciences, University of Nigeria, Nsukka*

Chemical bath deposition of semiconductor nanocrystalline thin films has been carried out within the pores of polyvinyl pyrrolidone (PVP) at room temperature. The chemical bath for the deposition of lead oxide is made up of lead acetate ($\text{Pb}(\text{CH}_3\text{COO})_2$), ammonia (NH_3) and PVP solution. The deposited films were annealed in the oven at a temperature of between 100°C and 300°C and characterized for the structural and optical properties. These properties were studied by means of X-ray diffraction (XRD) and optical spectrophotometer. XRD studies revealed the formation of nanocrystalline thin films. The results also show that high temperature annealing has significant effect on the structure and stoichiometry of lead oxide film deposited. From the absorption spectra, the band gap energy for lead oxide thin films lies in the range of $2.0 - 2.5\text{eV}$.

(Received April, 7, 2010; accepted August 12, 2010)

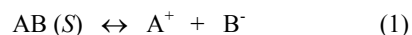
Keywords: CBD, Grain size, Optical properties, Stoichiometry, XRD

1. Introduction

Polymer capped inorganic thin film is the focus of many research groups [1 – 4]. For example, CdSe-polymer composites can be used to make blue light emitters [1]. Silver nanoparticles have been incorporated in the polyvinyl alcohol (PVA) matrix in order to improve its properties such as higher glass transition temperature and elastic [2]. Nanocrystalline thin films are also polycrystalline in nature but with sizes of crystallites of the order of a few nanometers. Extensive literature on size reduction effect is available [6 - 10]. Thin film deposition carried out within the pores of a polymer matrix has been reported as an effective means of modifying the sizes of the crystallites [6,7,11].

Chemical bath deposition is the technique used in this work. It was chosen because of its numerous advantages such as the simplicity and availability of apparatus, easier composition control, low processing temperature, lower cost, easier fabrication of large area films, easy process of complex shaped substrates and possibility of using high purity starting materials.

The theory behind chemical bath deposition (CBD) can be described as follows. Sparingly soluble salt, AB, when placed in water, a saturated solution containing A^+ and B^- ions in contact with undissolved solid AB is obtained and equilibrium is established between the solid phase and ions in the solution as [12]



Applying the law of mass action,

$$K = [\text{C}_A^+ \cdot \text{C}_B^-] / \text{C}_{\text{AB}}, \quad (2)$$

where C_A^+ , C_B^- and C_{AB} are concentrations of A^+ , B^- and AB in the solution, respectively. The concentration of pure solid is a constant number, i.e.

$$\text{C}_{\text{AB}}(\text{S}) = \text{constant} = K' \quad (3)$$

$$K = [\text{C}_A^+ \cdot \text{C}_B^-] / K', \quad (4)$$

$$K K' = \text{C}_A^+ \cdot \text{C}_B^- \quad (5)$$

Since K and K' are constants, the product of KK' is also constant, say K_s , therefore equ. (5) becomes:

$$K_s = \text{C}_A^+ \cdot \text{C}_B^- \quad (6)$$

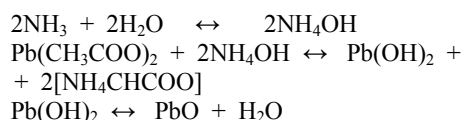
The constant, K_s , is called solubility product (SP) and ($\text{C}_A^+ \cdot \text{C}_B^-$) is called the ionic product (IP). When the solution is saturated, the ionic product is equal to the solubility product. But when the ionic product exceeds the solubility product, i.e. $\text{IP}/\text{SP} = S > 1$, the solution is supersaturated ($S = \text{degree of supersaturation}$), precipitation occurs and ions combine on the substrate and in the solution to form nuclei. Temperature, solvent and particle size affect the solubility product [13, 14]. Therefore, for thin film deposition to occur successfully, the ionic product must exceed the solubility product. A compound that is weakly soluble in water easily satisfies this condition. However, spontaneous precipitation should be eliminated in order for a thin film to form. This can be achieved by using an appropriate complexing agent, which can produce stable complex of the metallic ions in the solution. The complexing agent slowly releases the metal ions on dissociation, resulting in slow precipitation of the compound in the chemical bath by ion-ion reaction.

In this work, the reaction was slowed down and prevented from spontaneous precipitation by use of suitable complexing agents to form stable neutral complex ions, which then releases the ions slowly under a stable medium.

2. Experimental details

First the PVP solution was prepared by adding 400ml of distilled water to 4.0g of solid PVP and stirred by a magnetic stirrer without heating until the solution becomes homogeneous. This process lasted for one hour. The bath constituents for deposition of lead oxide thin films were lead acetate ($\text{Pb}(\text{CH}_3\text{COO})_2$) as a source of Pb^{2+} , ammonia (NH_3) as the complexing agent in a PVP medium. In a specific deposition set-up, the bath was composed of 10ml of 1M $\text{Pb}(\text{CH}_3\text{COO})_2$, 40ml of PVP solution and 6ml of NH_3 put in that order into 50ml beaker. Clean microslide was then inserted vertically through synthetic foam into the mixture. The deposition was allowed to proceed at room temperature for eight hours after which the coated substrate was removed, washed well with distilled water and allowed to dry.

The step-wise reaction involved in the complex ion formation and film deposition processes are given below.



Three of the deposited films were annealed in air at

N2(100°C), N3(200°C) and N4(300°C) for one hour. One of the samples, N1(as-grown) was left unannealed and used as control in order to study the effect of high temperature annealing on the deposited films.

3. Thin film characterization

The samples were characterized with XRD and UV-VIS Spectrophotometer. Optical properties of chemical bath deposited PVP-capped PbO nanocrystalline thin films were measured at room temperature by using Unico – UV-2102PC spectrophotometer at normal incident of light in the wavelength range of 200-1000nm. Optical band-gaps of the samples were calculated from the absorption spectra. The structure of the film was studied with X-ray diffractometer.

4. Results and discussions

4.1 Structural Analysis

X-ray diffraction (XRD) is an efficient tool for the structural analysis of crystalline materials. The XRD studies was carried out on all the samples deposited in this work using X'Pert HighScore PW1710 PANalytical Diffractometer, using the CuK_α radiation of wavelength $\lambda = 1.5408\text{\AA}$. The results are presented in figure 1. The existence of identifiable peaks in the diffractograms suggests that the films are highly crystalline in nature. However, the figures show that high temperature annealing has significant influence on the stoichiometry of the films deposited. Table 1 summarises the result from XRD analysis.

Table 1. Comparison of the results from XRD analysis of the films annealed at different temperature.

Annealing Temp.	Position (2 θ)	d-spacing	Compound Name	Chemical Formula	Ref. code
As-grown	28.96	3.08286	Lithargite	PbO	01-085-0711
„	35.80	2.50806	Lithargite	PbO	01-085-0711
„	38.60	2.33247	Oxygen	O ₂	00-038-0902
„	42.76	2.11306	Lithargite	PbO	01.085-0711
100°C	28.95	3.08399	Lead monoxide	PbO	00-038-1477
„	33.79	2.65283	Lead oxide	PbO ₂	00-050-1430
200°C	30.06	2.97290	Oxygen	O ₂	00-050-1381
„	36.17	2.48355	Lead	Pb	00-023-0345
300°C	38.38	2.34363	Oxygen	O ₂	00-038-0902

Table 1 shows that annealing the as-grown film in the oven at 100°C influences the structure of the film deposited, leading to the formation of film structure with different stoichiometry. In this case, lead oxide (PbO_2) appeared together with lead monoxide (PbO). There is also evaporation of oxygen off the film. However, annealing the film above 100°C leads to complete structural break down of the lead oxide formed. This result shows that lead oxide thin film deposited through chemical bath technique does not require high heat treatment for the formation of good crystalline film. This trend is similar to the report of

the work by D.D.O Eya. In his work, a more distinct and dense diffraction peaks were obtained for the films annealed at 130°C, which progressively decreased and became less distinct as the annealing temperature was increased [15].

The grain size (D) of the films under study was determined by measuring the full width at half maximum (β) using the Scherrer formula: $D = k\lambda / \beta \cos\theta$, where k is a constant taken to be 0.94, λ the wavelength of X-ray used ($\lambda = 1.5408\text{\AA}$) and θ is the Bragg's angle. Using Scherrer's formula, the grain sizes were found to be of the

order of 30nm and 73nm for the as-grown film and the film annealed at 100°C respectively. The number of crystallites per unit area (N) of the films was calculated from the formula, $N = t/D^3$, where t is the thickness of the film. The dislocation density (δ), defined as the length of dislocation lines per unit area, has been estimated using the equation, $\delta = 1/D^2$ [33]. The calculated structural parameters are summarized in Table 2.

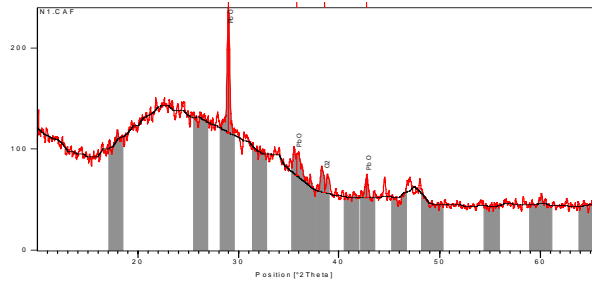


Fig.1a: XRD pattern of the as-grown film.

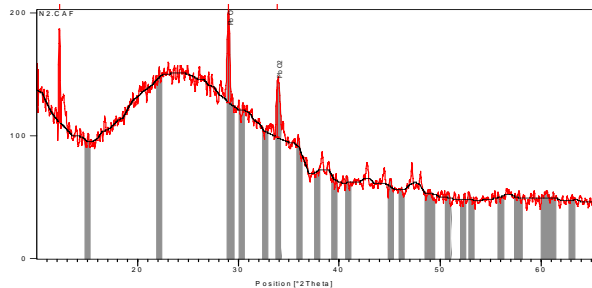


Fig.1b: XRD pattern of the film annealed at 100°C.

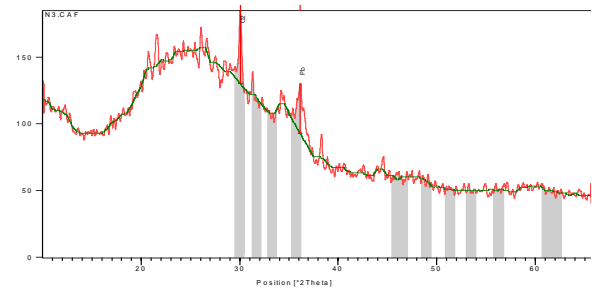


Fig.1c: XRD pattern of the film annealed at 200°C.

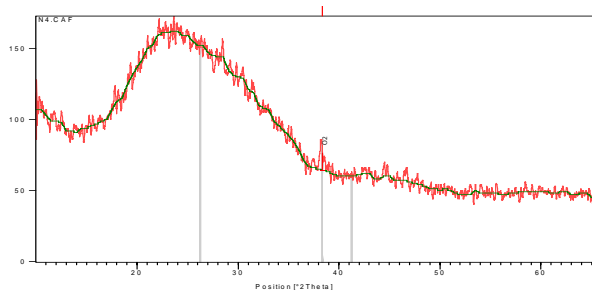


Fig.1d: XRD pattern of the film annealed at 300°C

4.2 The absorbance, transmittance, reflectance and refractive index of the films

The optical absorption spectra of the films deposited onto glass substrate were studied in the range of wavelengths 200 – 1000nm. Figure 2 shows the optical absorption as a function of the wavelength for the sample annealed at 100°C for one hour and the as-grown film. From this figure, it is found that lead oxide films deposited in this work absorb poorly in all three spectrum of solar light energy (UV-VIS-IR). However, the film has the highest absorbance of about 45% in the visible portion of the solar spectrum, corresponding to the film annealed at 100°C.

Table 2. Structural Parameter of Lead Oxide thin films annealed at different temperature

Annealing Temp.(°C)	Thickness (t) (nm)	Grain Size (D) (nm)	Number of Grains Per Unit Area (N) ($\times 10^{14}$)	Dislocation Density (δ) (line/m^2) ($\times 10^{14}$)
As-grown	264	30	97.800	11.11
100	255	73	6.600	1.88
200	244	42	32.900	5.67
300	238	13	0.001	59.17

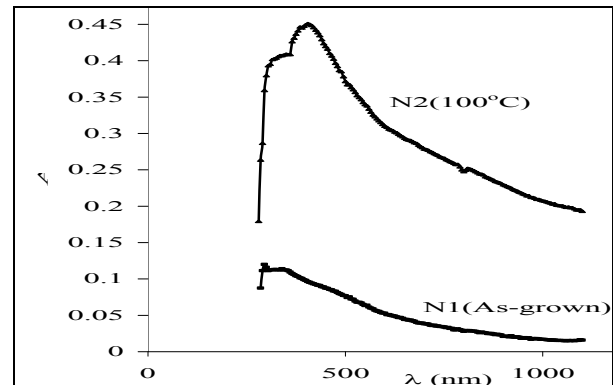


Fig. 2. Plot of absorbance vs. wavelength for lead oxide thin films.

The optical transmissions of as-grown and annealed lead oxide thin films are presented in figure 3. From the spectra, it is observed that the transmittance in the visible range is 90% for the as-grown and 52% for the film annealed at 100°C. The figure shows that thermal treatment lowers the optical transmittance of the films. The decrease in the transmittance with annealing temperature may have been caused by increase in grain size and the decrease in the number of defects that is associated with high temperature annealing of thin films [16]. By filling the voids in the film one expects denser

films and hence a decrease in the transmittance of the films.

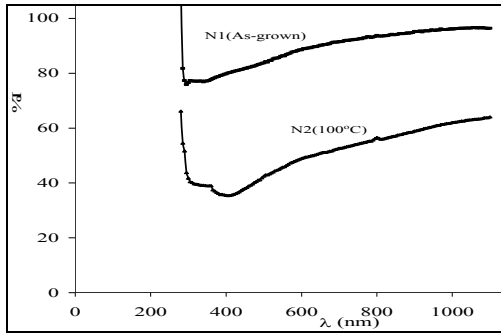


Fig. 2. Plot of transmittance vs. wavelength for lead oxide thin films.

Fig. 4 shows the spectral reflectance against wavelength for the samples under study. It can be observed that the annealed film has high reflectance (>18%) in both visible and NIR region of the solar spectrum.

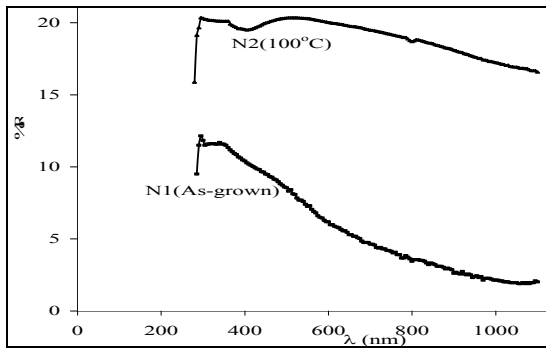


Fig. 4. Plot of reflectance against wavelength for lead oxide thin films

As shown in fig. 4, the refractive index (n) is calculated by the formula [17]

$$R = \frac{(n - 1)^2 + k^2}{(n + 1)^2 + k^2}$$

where R is the reflectivity of materials of refractive index, n and extinction coefficient, k. The variation of the refractive index with (hv) is shown in Fig. 5.

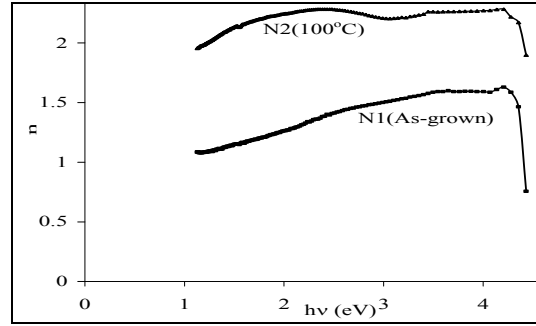


Fig. 5. Refractive index vs. hv for lead oxide thin films

The thin films with high transmittance and low reflectance are good material for antireflection coatings on transparent covers or windows of solar thermal devices to reduce reflectance, increase transmittance and improve their efficiencies. The high transmittance and low reflectance properties of the as-grown film are desirable characteristics for ideal solar control glazing to avoid glare problems and could be employed in solar thermal control coatings [18]. It has been shown that thin films refractive index lower than 1.9 could be employed as anti-reflecting material and could improve the transmittance of glass from 0.91 to 0.96 [19-20]. Again, the application of solar energy as a source of heat in chick brooding requires thin films with high transmittance in the NIR with moderate reflectance. The property of high transmittance in the NIR exhibited by the as-grown film therefore makes them good materials for the construction of poultry roofs and walls. This has the potential to minimize the cost of energy consumption associated with the use of electric bulbs, heater, stove etc and the hazards associated with them, while at the same time protecting the chicks from UV radiation.

4.3 Study of band gap as a function of photon energy

The details of the mathematical determination of absorption coefficient (α) can be found in literature [21] while the plots of absorption coefficient against photon energy is shown in fig. 6. The region of higher values of α , that is $\alpha > 10^4 \text{ cm}^{-1}$ correspond to transition between extended state in both valence and conduction bands while the lower values, that is $\alpha \leq 10^4 \text{ cm}^{-1}$ is the region where absorption present a rough exponential behaviour [22].

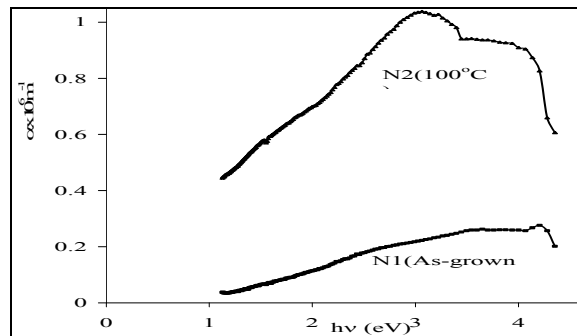


Fig. 6. Absorption coefficient vs. $h\nu$ for lead oxide thin film.

These absorption spectra, which are the most direct and perhaps the simplest method for probing the band structure of semiconductors are employed in the determination of the energy gap, E_g . The energy band gap (E_g) for the thin films deposited in this work was calculated using the following relation [23]:

$$\alpha = A(h\nu - E_g)^n / h\nu,$$

where A is a constant, $h\nu$ is the photon energy and α is the absorption coefficient, while n depends on the nature of the transition. For direct transitions $n = 1/2$ or $2/3$, while for indirect ones $n = 2$ or 3, depending on whether they are allowed or forbidden, respectively.

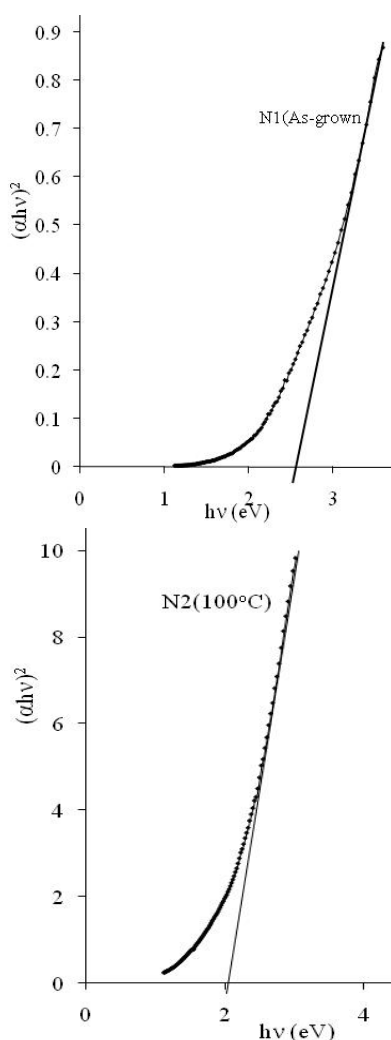


Fig. 7. $(ah\nu)^2$ vs. $h\nu$ for lead oxide nanocrystalline thin films.

The best fit of the experimental curve to a band gap semiconductor absorption function was obtained for $n = 1/2$. These graphs extrapolated to $h\nu$ axis give the values of E_g as 2.5eV for the as-grown film and 2.0eV for the film annealed in the oven at 100°C for one hour. A close observation of figure 7 shows that the energy gap decreased with increasing annealing temperature. This may be a consequence of the increase in crystallite size associated with high temperature annealing [16]. So the band gap decreases with annealing temperatures as a result of the increase in crystallite size based on the effective mass approximation: [24]

$$\Delta E_g = \hbar^2 \pi^2 / 2R^2 \{1/m_e + 1/m_h\} - (1.786e^2) / \epsilon R$$

where m_e , m_h are the effective masses of the electron in the conduction band and of the hole in the valence band respectively and ϵ is the static dielectric constant of the material. ΔE_g is the increase in band gap of the semiconducting material. The first term in the above equation represents the particle-in-a-box quantum localization energy and has simple $1/R^2$ dependence, where R is the particle radius; the second term represents the Coulomb energy with $1/R$ dependence. Hence, as R increases due to the increase in the crystallite size associated with high temperature annealing, the value of ΔE_g will go down. Literature survey show: (1) that processes that lead to increase in crystallite size decreases the band gap of most thin film semiconductors [6, 16, 25], (2) that a decrease in the energy band gap occurs, in most cases with post deposition annealing [27-29]. The direct band gap energy for the as-grown film obtained here compares well with the value 2.4eV reported in literature for PbO thin film annealed at 27°C [15].

A material with a direct band gap lower than 1.9eV has been regarded as a promising absorber for thin film photovoltaic applications [34]. Higher band gap value semiconductors are used as window layer in fabrication of solar cell. The high band gap energy of lead oxide thin films deposited in this work make the films ideal for use as window materials in solar cell fabrication.

4.4 Extinction coefficient, real and imaginary dielectric constant

The extinction coefficient (k) is related to absorption coefficient (α) by the relation [29-30]:

$$k = \frac{\alpha \lambda}{4\pi}$$

Similarly, the dielectric constant is related to n and k by the relations [31-32]:

$\epsilon_r = n^2 - k^2$ for the real part, and $\epsilon_i = 2nk$ for imaginary part.

The variation of the extinction coefficient k, real, ϵ_r and imaginary, ϵ_i part of the dielectric constant with photon energy for the films under study are shown in figs. 8, 9 and 10 respectively.

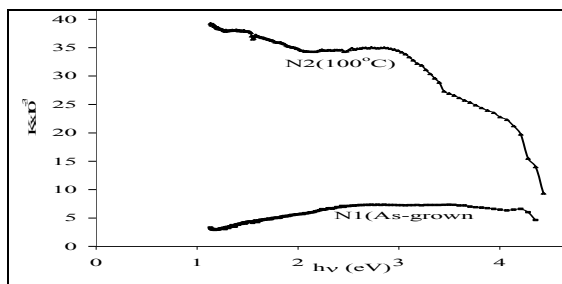


Fig. 8. Extinction coefficient vs. photon energy for lead oxide thin films.

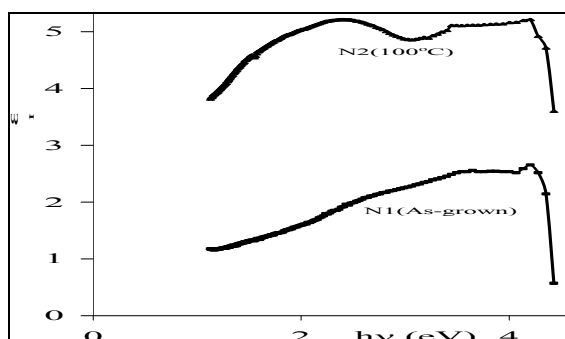


Fig. 9. Real dielectric constant vs. photon energy for lead oxide thin films.

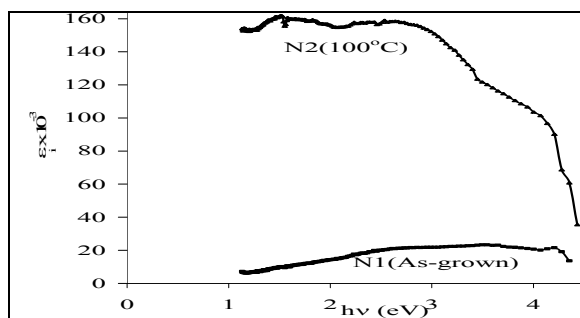


Fig. 10. Imaginary dielectric constant vs. photon energy for lead oxide thin films.

5. Conclusion

This study focuses on the synthesis and structural and optical characterization of thin films of lead oxide. The films were deposited by chemical bath deposition technique and annealed at different temperature. XRD study reveals that highly crystalline lead oxide thin films synthesized by chemical process could be obtained at a relatively low annealing temperature. Increasing the annealing temperature changes the stoichiometry of the film deposited. Optical studies and band gap analysis show also that high temperature annealing has significant effect on these properties.

Reference

- [1] X. Lu, L. Li, W. Zhang, C. Wang; *Nanotechnology* **16**, 2233 (2005)
- [2] B. O. Dabbousi, M.G Bawendi, O. Omtduku, M. F. Rubne; *Appl. Phys. Lett.* **66**, 1326 (1996)
- [3] Z. H. Mbele; *Chem. Mater.* **15**, 5019(2003)
- [4] M.Pattabi, B.S Amm and K. Manzoor; *Mater.Res. Bull.* **42**, 828 (2007)
- [5] K. Pato, E. Swatsitang, W.Jareonboon, S. Maensiri, V. Promarak; *Optoelectron. Adv. Mater.-Rapid Comm.* **1**, 287(2007)
- [6] S. Jana, R. Thapa, R. Maity, K. K. Chattopadhyay; *Physica E* (2008) doi: 10.1016/j.physe.2008.04.015
- [7] P. K Ghosh, S. Jana, U. N Maity, K. K. Chaltopadhyay; *Physica E* **35**, 178 (2006)
- [8] W. Lou, X. Wang, M. Chen, W. Liu, J. Hao; *Nanotechnology* **19**, 225607 (2008)
- [9] J. P. Cheng, X. B. Zhang, Z. Q. Luo; *Surface and coatings Tech.* **202**, 4681 (2008)
- [10] D. S. Dhawale, A. M. More, S. S. LAtthe, K. Y. RAjpure, C.D. Lokhande; *Applied Surface Science* **254**, 3269 (2008)
- [11] P. M. Rorvik, A Almli, A. T. J. Helvoort, R. Holmestad, T. Tybell, T. Grande, M. Einarsrud; *Nanotechnology* **19**, 225605 (2008)
- [12] H. M. Pathan, C. D. Lokhande, *J. Bull Mater.Sc* **27**, 85 (2004)
- [13] D. J. Skoog, D. M. West, *Fundamental of Analytical Chemistry* (Holt Rinehart and Winston) 2nd e.d
- [14] D. Lincot, R. O. Borges, *J. Electrochem. Sos* **139**, 1880(1992)
- [15] D. D. O. Eya, *The Pacific J. Sci. and Techno.*, **7**(2), 144 (2006)
- [16] S. Erat, H. Metin, CP899, Sixth International Conference of the Balkan Physical Union, edited by S.A. Cetin and I. Hikmet, 249 (2007)
- [17] G. Hass, J.B. Heaey, W.R. Hunter, *Physics of Thin Films* Ed. G. Hass, M. H. Francombe, J. L. Vassen, Academic Press, New York **12**, 1 (1982)
- [18] P. K. Nair, M. T. S. Nair, A. Femaardex, M. J. Ocampo, *Phys. D: Appl. Phys.* **22**, 829 (1989)
- [19] C. J. Brinker, M.S. Harrington, *Solar Energy Materials*, **52**, 159 (1981)
- [20] R. B. Petit, C. J. Brinker, *Solar Energy Materials*, **14**, 269 (1986)
- [21] F. I. Ezema, *Turk J. Physics*, **29**, 105 (2005)
- [22] M. F. Kotkata, M. T. El-Shair, M. A. Afifi, M. M. A. Azizi, *J. Phys. D: Appl. Phys.*, **27**, 623 (1994)
- [23] V. Estrella, M.T.S. Nair, P.K. Nair; *Thin Solid Films*, **414**, 289 (2002)
- [24] A. Popa, M. Lisca, V. Stancu, M. Buda, E. Pentia, T. Botila, *J. Optoelectron. Adv. Mater.* **8**(1), 43 (2006)
- [25] A. Djelloul, K. Bouzid, F. Guerrab, *Turk J. Phys.* **32**, 1(2008)
- [26] D. Soubane, A. Ihlal and G. Nouet, *M.J. Condensed*

- Matter, **9**(1), 32(2007).
- [27] F. I. Ezema, S.C. Ezugwu, R.U. Osuji, P.U. Asogwa, B.A. Ezekoye, A.B.C. Ekwealor, M.P. Ogbu, J. of Non-Oxide Glasses, **1**(1), 45(2010)
- [28] S. G. Kandalkar, C. D. Lokhande, R. S. Mane, S. H. Han, Appl. Surf. Sci. **253**, 3952(2007)
- [29] A. Arias-Carbajal Readigos, V. M. Gearcia, O. Gomezdaza, J. Campos, M. T. S. Nair, P. K. Nair, Semicond. Sci. Technol. **15**, 1022(2000)
- [30] I. M. Tsidilkovsk, Band structure of semiconductors, Pergamon Press, Oxford (1982)
- [31] J. I. Pankove, Optical processes in semiconductors, Prentice-Hall, New York (1971)
- [32] I. C. Ndukwe, Sol. Ener. Mater. Sol. Cells **40**, 123 (1996).
- [33] K. Ravichandran, G. Muruganatham, B. Sakthivel, P. Philominathan, J. of Ovonic Research, **5**(3), 63 (2009).
- [34] T. Watanabe, M. Matsui ; J. Appl. Phys. **38**, 1379 (1999)

*Corresponding author: sabroec@gmail.com,
sabro2e@yahoo.com